Object Localization with Multiple Sensors

Shashank Shekhar
Oussama Khatib
Makoto Shimojo*

Robotics Laboratory
Computer Science Department
Stanford University
Stanford, California

Abstract

We present a method to obtain the position and orientation of an object through measurement from multiple sensors. Raw sensor measurements are subject to limitations of sensor precision and accuracy. Although for most measurements the estimate of position parameters is a linear function of the measurements, the estimate of orientation parameters is a nonlinear function of the measurements. Thus, error in orientation estimate depends on the distance over which the raw measurements are made. For example, the estimate of the orientation of a line is better, the farther apart two points on the line are. The problem of finding the orientation parameters is formulated in two steps. The first step computes vectors from sensor measurements of points. A concept of best features *is developed to select an optimal set of all possible vectors. The second step relates the orientation parameters to the vectors from the first step as a linear system. The best estimate is obtained by solving a weighted linear system of the optimal set of vectors in a least squares sense. The optimal selection of best features improves the estimate substantially. This method has been implemented for localizing an object in a manipulator end-effector instrumented with centroid and matrix tactile sensors.*

1. Introduction

An important characteristic of robots aimed at accomplishing advanced tasks is their ability to ascertain the state of their workspaces. The uncertainties in the position and orientation of an object with respect to a manipulator are primarily due (Brooks 1982) to placement error in the position and orientation of the object in the workspace, dimensional tolerance in the object, and positioning error of the robot. Such uncertainties cannot be recovered prior to actual operation. A robust assembly program will generate actions that depend on real-time sensory information. Expected errors in such sensory information will also allow an assembly planning system to determine if an operation will eventually succeed.

The problem of locating an object using sensory information has so far received attention only as a part of the problem of object recognition. Grimson and Lozano-Perez (1984) proposed a solution using simple geometric relations based on pairs of observations. Faugeras and Hebert (1983) presented a least squares estimation method for the position and orientation obtained from redundant measurements. Bolle and Cooper (1986) considered combining pieces of feature estimates to obtain the estimate of position and orientation of an object. Since the method involves a nonlinear optimization algorithm, it is not suitable for real-time implementation. Also, measurements are weighted at the level of derived features (*i.e.*, lines, planes). This method, therefore cannot account for sensor inaccuracies at the level of subfeature or device measurements. In the context of task level specification, a symbolic solution for the position and orientation based on spatial relationships was proposed by Popplestone, Ambler, and Bellos (1980) in indeterminate situations.

In this paper, we present a method for an optimal estimation of the position and orientation parameters of an object. The optimality is taken in the sense of least expected error on the estimates. The parameter estimation is generally a two-step process. First, device measurements are combined to obtain intermediate parameters. Then the final parameters are obtained from a system of equations on the intermediate parameters. For example, to find the orientation of an

* Author's present address: Industrial Products Research Institute, 1-1-4 Yatabe-Machi Higashi, Tsukuba-Gun, Ibaraki 305, Japan.

The International Journal of Robotics Research,
Vol. 7, No. 6, December 1988,

object, device measurements of some points are first combined to obtain estimates of vectors and then the orientation is obtained from a system of equations on these vectors. If the device measurements are more than the least required for a unique solution of an intermediate parameter, several estimates of the intermediate parameter are possible. We show that an appropriate selection of intermediate parameters improves the expected estimate of the final parameters. This set of best intermediate parameters is called the set of *best features*. The set accounts for all individual device measurements. The optimal estimate is obtained by solving the system of *best features* in a weighted least squares sense. We also determine bounds on the errors. Finally, we describe the application of this method to the localization of an object in a two-fingered, two-degree-of-freedom end-effector using two pressure-conductive rubber centroid sensors and a matrix tactile sensor.

The formulation of object localization problem is presented in Section 2. Section 3 describes the proposed procedure to obtain the position and orientation parameters. A brief overview of the sensors follows in Section 4. The error characteristic of the individual sensors, the localization experiment, and the results are presented in Section 5.

2. Localization Problem

The position and orientation of an object is obtained by relating the sensor measurements to some a priori known dimension of the object. First, the relationship between the sensor measurements and object dimensions is established. The correspondence between sensor measurements and object dimensions is assumed to be given. Then the concept of *best features* is developed.

2.1. Measurements

Device (raw) measurements are characterized by their precision and reliability. A sensor precision is the built in ability to resolve measurements. Reliability is the measure of systematic errors. Both errors are combined to characterize the device measurements in the form $m \pm \Delta m$.

2.2. Position and Orientation

To a sensor measurement of an identifiable feature of the object, there is a corresponding measure of that feature in the object's model. Objects have six degrees of freedom with respect to the sensors. Thus,

$$^{s}\mathbf{p}_k = \mathbf{R}\,{}^{o}\mathbf{p}_k + \mathbf{h} \tag{1}$$

represents the relationship of the kth point $^{o}\mathbf{p}_k$ described in the object frame of reference to its description $^{s}\mathbf{p}_k$ in the sensor frame. $\mathbf{R}$ is the 3×3 rotation transformation matrix, and $\mathbf{h}$ is the position vector of the origin of the object frame in the sensor frame. We will assume that all sensor measurements are described in a measurement reference frame. Given sensor measurements $^{s}\mathbf{p}_k$'s and corresponding values of $^{o}\mathbf{p}_k$'s from the object model, there are three position and three orientation parameters to solve for. The orientation components and the position components are solved independently. The orientation is evaluated from

$$^{s}\mathbf{v}_i = \mathbf{R}\,{}^{o}\mathbf{v}_i, \tag{2}$$

where $^{s}\mathbf{v}_i$ and $^{o}\mathbf{v}_i$ are either vectors obtained from one sensor measurement or from points, such as

$$^{s}\mathbf{v}_i = (^{s}\mathbf{p}_k - {}^{s}\mathbf{p}_l), \qquad {}^{o}\mathbf{v}_i = (^{o}\mathbf{p}_k - {}^{o}\mathbf{p}_l).$$

The elements of $\mathbf{R}$ in any of the three commonly used representations — Euler angle representation; roll, pitch, yaw representation; and axis-angle representation — must be solved with the condition that $\mathbf{R}^{\mathrm{T}}\mathbf{R} = \mathbf{I}$, where $\mathbf{I}$ is a 3×3 identity matrix. There are nine unknowns with six quadratic constraints. Using quaternions, we can reduce the problem of orientation estimate to finding the solution of a linear system with one normality condition on Euler parameters. A brief review of quaternions is presented in the Appendix.

The position parameters are evaluated from a scalar equation on the distance. To a given distance measurement ${}^{s}d_i$ in the sensor along a direction ${}^{s}\mathbf{n}_i$ there is a corresponding distance ${}^{o}d_i$ in the model computed along ${}^{s}\mathbf{n}_i$. These two measurements are related by (Faugeras and Hebert 1983)

$$ {}^{s}\mathbf{n}_i^{T}\,\mathbf{h} = {}^{s}d_i - {}^{o}d_i. \tag{3} $$

For the orientation, at least two independent vectors are required to uniquely determine the orientation parameters. The position estimate requires the measurement of at least one vertex or three nonparallel planes. However, there are often more measurements than the least required for a unique solution. In such cases measurements can be tested against their contribution to the error in the solution.

2.3. Best Features

Let us consider the problem of estimating the orientation of a quadrangle object in a plane. For the purpose of this example, assume that all points are measured with the same device error. Let us order pairs of points based on their distance. Of these pairs select the set of pairs with the largest distance such that all measurements are accounted for at least once. The estimate of the angle based on these pairs has the least maximum expected error. The following example illustrates it numerically.

The object shown in Fig. 1 has vertices *A*, *B*, *C*, and *D* located at (0, 0), (5, 11), (100, 0), and (50, − 11). All vertices are measured with an uncertainty of ± 3 units. One possible configuration of the measured shape is shown in dotted lines. The estimate of the angle can be obtained by comparing just one or several pairs of vertices to their corresponding feature in the model. For instance based on the selection of *AB*, *BC*, *CD*, and *DA*, the weighted least squares estimate of the angle has $\pm 9°$ of expected maximum error (as given by Eq. (19)). Now, let us arrange pairs of vertices by decreasing distance: *AC*, *BC*, *CD*, *DA*, ... In order to make use of all the measurements, at least three distinct pairs of vertices are necessary. The expected maximum error on the angle estimate based on the first three pairs (*AC*, *BC*, *CD*) is $\pm 3°$. This estimate is the best estimate considering all measurements at least once. Since device errors are identical, the expected error on the estimate is inversely proportional to the distance between vertices. The three pairs with the largest distance have the least expected error. It can be shown that any other combination of three or more pairs has a larger maximum expected error.

Fig. 1. Selection of measurement. The potential features that can be matched are AB, BC, CD, DA, AC, and BD. Selection of AC, BC, and CD give least expected error in orientation estimate.

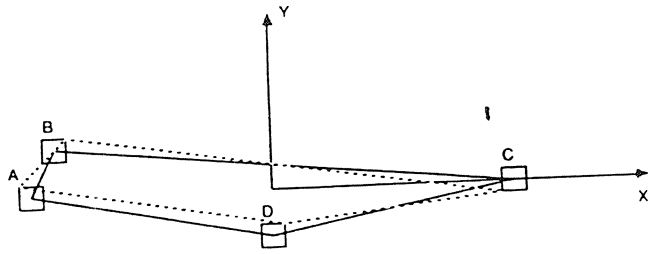

This example illustrates the two-step process in estimating the orientation of the object:

1. Select the optimal set of independent intermediate parameters.
2. Solve for final parameters in a weighted least squares sense.

The selection of intermediate parameters is based on their expected errors. The optimal set of such independent intermediate parameters that accounts for all device measurements is called the set of *best features*. In the previous example, the set of *best features* consisted of (*AC*, *BC*, *CD*).

3. Localization Procedure

In this section we describe the proposed algorithm to obtain the position and orientation parameters. A weighting function for the weighted least squares estimate is proposed and the solution of the linear system is presented. We also determine bounds on the expected errors.

Fig. 2. Angular uncertainty.

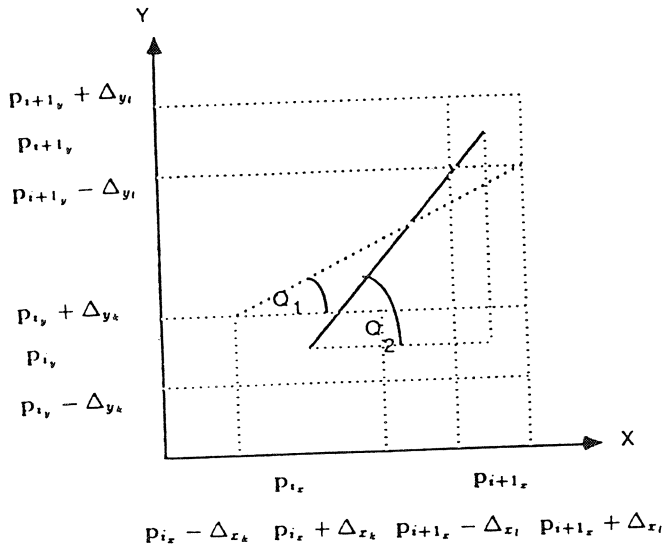

3.1. Orientation Estimate

The orientation is estimated from a set of vectors. First, we determine the expected error on the estimate of each vector. Based on this error, the set of *best features* is selected. The expected errors are also used to determine the weighting function.

3.1.1. Weighting Function

Let ${}^s\mathbf{v}_i$ be the estimate of the vector ${}^o\mathbf{v}_i$ obtained from device measurements of the vertices $\mathbf{p}_i$ and $\mathbf{p}_{i+1}$. Let Δ_j be the bounding error on the position measurement obtained from the jth sensor. The largest expected error on the estimate ${}^s\mathbf{v}_i$ can be defined by a vector $\delta\Phi_i$. The procedure to obtain $\delta\Phi_i$ is described as follows. Let us assume that the vector ${}^s\mathbf{v}_i$ has been obtained from vertices measured by sensors k and l. Given sensor errors, the actual position of the vertices lie within the cubes Δ_k and Δ_l correspondingly. The vector $\delta\Phi_i$ is computed by considering the largest deviation of ${}^s\mathbf{v}_i$ within the cubes. For instance, the z-component is computed as follows (see Fig. 2):

$$\begin{aligned}\delta\phi_{z_i} &= \phi_2 - \phi_1 \simeq \tan(\phi_2 - \phi_1) \\ &= \frac{v_{y_i}(v_{x_i} + \Delta v_{x_i}) - v_{x_i}(v_{y_i} - \Delta v_{y_i})}{v_{x_i}(v_{x_i} + \Delta v_{x_i}) + v_{y_i}(v_{y_i} - \Delta v_{y_i})}\end{aligned} \tag{4}$$

where

$$\Delta v_{x_i} = \Delta_{x_k} + \Delta_{x_l}, \qquad \Delta v_{y_i} = \Delta_{y_k} + \Delta_{y_l}.$$

The components $\delta\phi_{x_i}$ and $\delta\phi_{y_i}$ can be similarly obtained.

An estimate of the orientation can then be characterized by the magnitude $\delta\Phi_i^T\,\delta\Phi_i$. A selection procedure based on these magnitudes will determine the set of *best features*. Let n be the number of vertices. There are $\binom{n}{2}$ possible vectors from combinations of vertices where $\binom{\ }{\ }$ is binomial coefficient operator. However only $n-1$ vectors are sufficient to account for all the measurements. The set of *best features* consists, therefore, of only $n-1$ vectors. The *weighting function* is defined by the scalar $\delta\Phi_i^T\,\delta\Phi_i$.

3.1.2. Orientation Parameters

After the set of *best features* is selected, the estimation problem is formalized as a linear system of equations based on the vectors in this set. This system is then solved using a weighted left inverse matrix.

Let $\mathbf{R}$ be the transformation relating vectors ${}^s\mathbf{v}_i$ and ${}^o\mathbf{v}_i$ as given in Eq. (2). Using the quaternion ($\mathbf{q} = (u_0, \mathbf{u})$) corresponding to the transformation $\mathbf{R}$, the relationship between these vectors becomes (see Appendix)

$${}^s\mathbf{v}_i = \mathbf{q}\,{}^o\mathbf{v}_i\mathbf{q}^*,$$

which can be rewritten as

$${}^s\mathbf{v}_i\mathbf{q} = \mathbf{q}\,{}^o\mathbf{v}_i. \tag{5}$$

Equating the scalar and vector parts of this equation yields

$$({}^s\mathbf{v}_i + {}^o\mathbf{v}_i) \times \mathbf{u} = u_0({}^o\mathbf{v}_i - {}^s\mathbf{v}_i), \tag{6}$$

$$\mathbf{u} \cdot ({}^s\mathbf{v}_i - {}^o\mathbf{v}_i) = 0. \tag{7}$$

If ${}^s\mathbf{v}_i + {}^o\mathbf{v}_i$ is a nonzero vector, the orientation parameters can be completely determined from Eq. (6). In case ${}^s\mathbf{v}_i + {}^o\mathbf{v}_i$ is zero, the object frame relative to the sensors can be selected arbitrarily so that ${}^s\mathbf{v}_i + {}^o\mathbf{v}_i$ is nonzero. So, using Eq. (6), express it as a linear system

$$\mathbf{A}_i\mathbf{u} = u_0\mathbf{b}_i, \tag{8}$$

where A_i is the cross-product operator of ${}^s\mathbf{v}_i + {}^o\mathbf{v}_i$ and $\mathbf{b}_i$ is the vector ${}^o\mathbf{v}_i - {}^s\mathbf{v}_i$. The system of equations for multiple estimates is

$$\mathbf{A}\mathbf{u} = u_0\mathbf{b}, \tag{9}$$

where

$$\mathbf{A} = [\mathbf{A}_1^T, \mathbf{A}_2^T, \ldots, \mathbf{A}_n^T]^T,$$
$$\mathbf{b} = [\mathbf{b}_1^T, \mathbf{b}_2^T, \ldots, \mathbf{b}_n^T]^T.$$

The weighting matrix for each estimate is defined as

$$\mathbf{W}_{r_i} = w_{r_i}^2\mathbf{I}, \tag{10}$$

where $w_{r_i} = 1/(1 + \delta\Phi_i^T\,\delta\Phi_i)$ and $\mathbf{I}$ designates the 3×3 identity matrix.

The weighted system of equations is

$$\mathbf{W}_r\mathbf{A}\mathbf{u} = u_0\mathbf{W}_r\mathbf{b}, \tag{11}$$

where

$$\mathbf{W}_r = \text{diag}\,(\mathbf{W}_{r_i}).$$

Using the normality condition of Euler parameters, we obtain the solution of the system

$$u_0 = 1/\sqrt{1 + \mathbf{g}^T\mathbf{g}}, \qquad \mathbf{u} = u_0\mathbf{g} \tag{12}$$

where

$$\mathbf{g} = \mathbf{G}\mathbf{b} \tag{13}$$

and G represents the weighted left inverse matrix

$$\mathbf{G} = (\mathbf{A}^T\mathbf{W}_r\mathbf{A})^{-1}\mathbf{A}^T\mathbf{W}_r. \tag{14}$$

The rotation matrix R corresponding to the solution $\mathbf{q} = (u_0, \mathbf{u})$ of Eq. (12) is given by (Khatib 1980)

$$\mathbf{R} = \begin{bmatrix} 2(u_0^2 + u_1^2) - 1 & 2(u_1u_2 - u_0u_3) & 2(u_1u_3 + u_0u_2) \\ 2(u_1u_2 + u_0u_3) & 2(u_0^2 + u_2^2) - 1 & 2(u_2u_3 - u_0u_1) \\ 2(u_1u_3 - u_0u_2) & 2(u_2u_3 + u_0u_1) & 2(u_0^2 + u_3^2) - 1 \end{bmatrix}. \tag{15}$$

3.1.3. Orientation Error Vector

We have determined the estimate of the orientation of the object in a weighted least squares sense. The error associated with a vector ${}^s\mathbf{v}_i$ has been defined by the elementary rotation vector $\delta\Phi_i$ (see Eq. (4)). To an elementary rotation vector $\delta\Phi_i$ corresponds an elementary variation $\delta\mathbf{q}_i$ given by (Khatib 1980)

$$\delta\mathbf{q}_i = \tfrac{1}{2}\check{\mathbf{q}}\,\delta\Phi_i, \tag{16}$$

where

$$\check{\mathbf{q}} = \begin{bmatrix} -u_1 & -u_2 & -u_3 \\ u_0 & u_3 & -u_2 \\ -u_3 & u_0 & u_1 \\ u_2 & -u_1 & u_0 \end{bmatrix}. \tag{17}$$

The orientation estimate q lies within $\mathbf{q} \pm \delta\mathbf{q}$. The error vector $\delta\mathbf{q}$ is determined by considering the contribution of $\delta\mathbf{q}_i$'s from each vector in the same weighted least squares sense

$$\delta\mathbf{q} = \sum_i w_{r_i}^2\,\delta\mathbf{q}_i \Big/ \sum_i w_{r_i}^2. \tag{18}$$

From (16) the equation becomes

$$\delta\mathbf{q} = \tfrac{1}{2}\check{\mathbf{q}}\sum_i w_{r_i}^2\,\delta\Phi_i \Big/ \sum_i w_{r_i}^2. \tag{19}$$

3.2. Position Estimate

The object position can be obtained from Eq. (3) which involves measurement of vertices or distances of planes to the origin.

3.2.1. Weighting Scheme, Position Parameters and Error Vector

Let $\{\delta d_i\}$ be the position measurement error. The weighting function is selected as $w_{pi} = 1/(1 + \delta d_i^2)$. The position parameters are linear functions of distance measurements as defined in Eq. (3). For multiple measurements, Eq. (3) becomes

$$\mathbf{C}\mathbf{h} = \mathbf{d}, \tag{20}$$

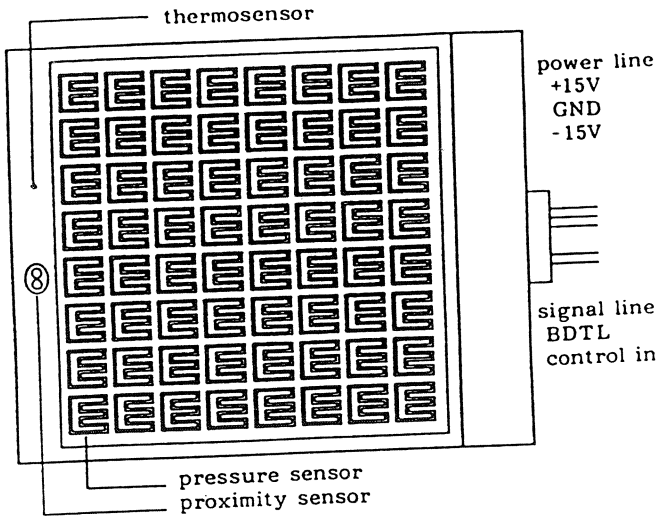

Fig. 3. Structure of matrix tactile sensor.

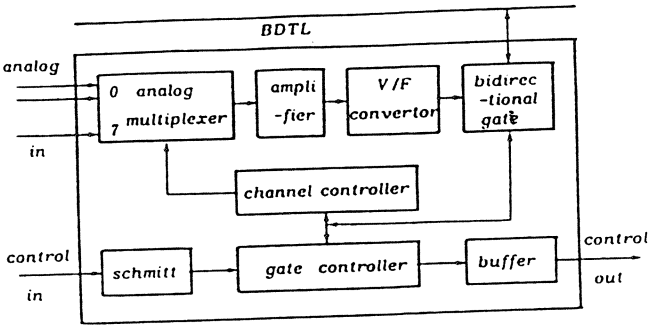

Fig. 4. Transmission element of hybrid IC.

where

$$\mathbf{C} = [{}^{s}\mathbf{n}_1, {}^{s}\mathbf{n}_2, \ldots, {}^{s}\mathbf{n}_2]^{\mathrm{T}},$$
$$\mathbf{d} = [d_1, d_2, \ldots, d_n]^{\mathrm{T}}.$$

The weighted system of equations is

$$\mathbf{W}_p\mathbf{C}\mathbf{h} = \mathbf{W}_p\mathbf{d},$$

where

$$\mathbf{W}_p = \mathrm{diag}\,(w_{p_i}).$$

The solution is

$$\mathbf{h} = \mathbf{P}\,\mathbf{d}, \tag{21}$$

where

$$\mathbf{P} = (\mathbf{C}^{\mathrm{T}}\mathbf{W}_p\mathbf{C})^{-1}\mathbf{C}^{\mathrm{T}}\mathbf{W}_p.$$

The error on the estimate of the position is given by

$$\delta\mathbf{h} = \mathbf{P}\,\delta\mathbf{d}, \tag{22}$$

where

$$\delta\mathbf{d} = [\delta d_1, \delta d_2, \ldots, \delta d_n]^{\mathrm{T}}.$$

4. Sensor Description

A matrix tactile sensor and two centroid sensors have been mounted on the end-effector. We include a review of the sensor's working principles and characteristics. A more detailed description can be found in Ishikawa and Shimojo (1982) and Shimojo and Ishikawa (1985a,b).

4.1. Matrix Tactile Sensor

The matrix tactile sensor has 8×8 elements each of 5 mm^2 dimension. Its output is pressure distribution information on a gray scale. In addition, it has one output each from a proximity sensor and a thermal sensor. A feature of the sensor is reduction of signal wires from detectors by using a transmission element.

4.1.1. Working Principle and Characteristics

Pressure measurement is based on change in resistivity of a thin pressure conductive rubber mounted on the surface. The change in resistivity is measured through a gold plated electrode pattern, as shown in Fig. 3, etched on the surface of the circuit board. The sensor has a transmission element mounted at the back for multiplexing the 66 analog outputs of the array over a single channel in frequency modulated form. Figure 4 shows a block diagram of the transmission element which has been made as a hybrid IC. It has an eight-

Table 1. Specification of Transmission Element

Item	Specifications
Analog input	8 channel/TE, range: 0 to +15 V
Scan speed	50 μs/channel
Modulation method	Pulse frequency modulation
Electrical element	CMOS, Transistor, Diode
Power supply	±15 V GND
Power dissipation	45 mW(typ) 90 mW (max)
IC type	Thick Film Hybrid IC
Dimension	35 mm (w) × 22 mm (h) × 5.5 mm (t)
Package	Single in Line

channel analog multiplexer, a V/F converter and a control circuit. Each sensor is an element. Any number of elements can be connected by connecting "control in" and "control out" pin of the elements serially. Table 1 shows the specification of the transmission element.

4.2. Centroid Sensor

The centroid sensor outputs the center of pressure of a two-dimensional pressure distribution and the total force applied. Since the sensor is made of thin material, it is pliable and has sheetlike form. It can be mounted on curved surfaces (i.e., cylindrical fingers). The center of pressure and total force output are direct and do not require any computational effort. The sensor needs only four wires. As the output impedance is low (≈ 100 kΩ), the sensor is robust for electrical noise.

4.2.1. Working Principle and Characteristics

As shown in Fig. 5, the sensor has a three-layered structure. Layers A and B are made of electrically conductive material coated film. Layer S is made of pressure conductive rubber. The resistance $r_p(x, y)$ of the rubber along the thickness varies according to the pressure distribution. The boundary of the sensor divided into S_1, S_2, S_3, S_4 is surrounded by electrodes

Fig. 5. Structure of the centroid sensor. 1. Resistive material coated film. 2. Pressure conductive rubber. 3. Electrode.

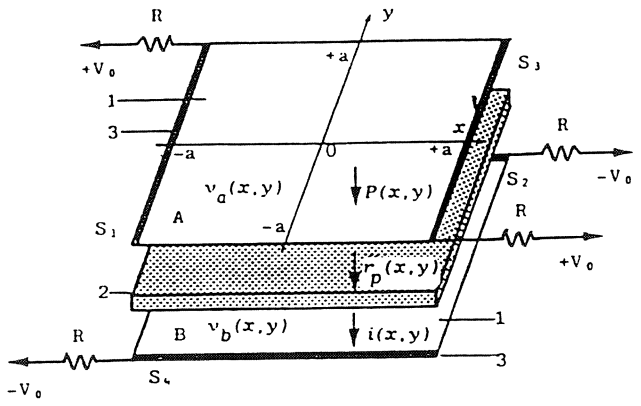

that contact with layer A or B and connect to constant voltage sources V_0 via resistor R.

The drop in resistance $r_p(x, y)$ of the rubber due to a pressure distribution causes a current distribution $i(x, y)$ proportional to the resistance drop. The current density induces a voltage distribution $v(x, y)$ on the surface of layers A and B. The current density and the induced voltage are related through Poisson's equation

$$\nabla^2 v = ri \qquad \left(\nabla^2 = \frac{\partial^2}{\partial x^2} + \frac{\partial^2}{\partial y^2}\right), \tag{23}$$

where r is surface resistance in the layer A and B. The first order moments of the current density distribution I_x, I_y in the cartesian coordinates and the total current I are given by

$$I_x = \int\int_D xi(x, y)\, dx\, dy, \tag{24}$$

$$I_y = \int\int_D yi(x, y)\, dx\, dy, \tag{25}$$

$$I = \int\int_D i(x, y)\, dx\, dy. \tag{26}$$

With rectangular sensor boundary conditions on Eq. (23), the following expressions are obtained:

$$I_x = a\left(\frac{1}{R} + \frac{2}{r}\right)([v_A]_{S_1} - [v_A]_{S_3}), \tag{27}$$

Fig. 6. Pressure response of conductive rubber.

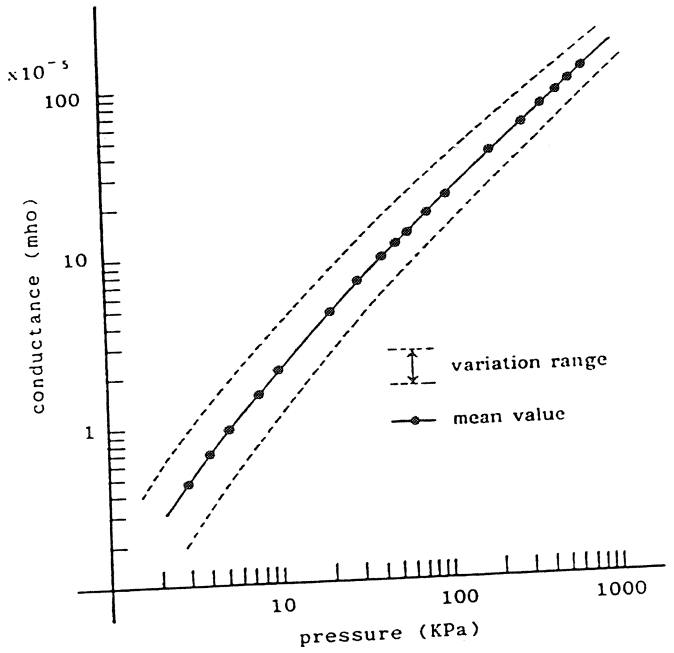

Fig. 7. Outputs of sensor versus pressed position.

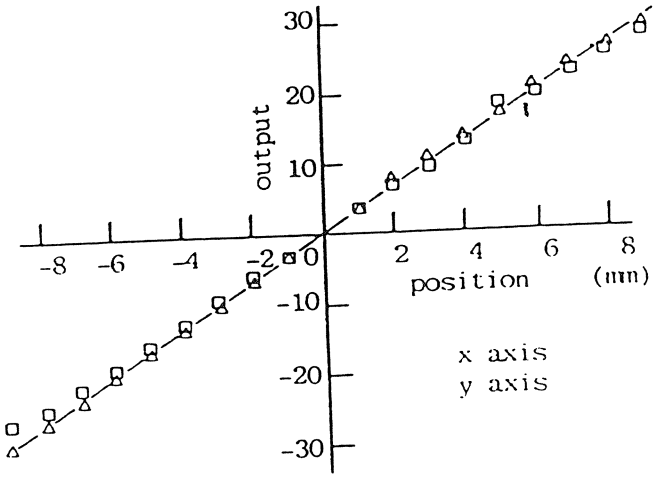

$$I_y = a\left(\frac{1}{R} + \frac{2}{r}\right)([v_B]_{S_2} - [v_B]_{S_4}), \tag{28}$$

$$I = \frac{2V_0 - [v_A]_{S_1} - [v_A]_{S_3}}{R}. \tag{29}$$

The total force is derived from Eq. (29) and with known relation between current distribution and the pressure distribution, Eqs. (27), (28), and (29) give the center of pressure.

5. Experimental Results

The error estimate of each sensor was measured experimentally. These estimates are presented in Section 5.1. The error estimates and the physical configuration of the sensors determine the accuracy of localization process. We present in Section 5.2 the experimental setup and a summary of the results in localizing an object in a two-finger gripper.

5.1. Sensitivity and Localization of Sensors

In the first experiment, the characteristics of the pressure conductive rubber used in the sensors were measured. The distributed pressure was quasistatically loaded with a right cylinder 6 mm in diameter, and the load was measured by a semiconductor force transducer. As shown in Fig. 6, the change in resistivity r_p varies polynomially with the pressure; i.e., $r_p \propto p^{-1.9}$.

In the next experiment, the localization error of the centroid sensor was measured. The centroid sensor measures 30 × 40 mm. Under conditions similar to the previous experiment, the outputs of the sensor in both x and y directions were measured along with the actual location of the probe. As shown in Fig. 7, the outputs of the sensor in both x and y directions are plotted against the probe location. The error in center of pressure is bounded by 1.0% of the size of the sensor in that direction (i.e., ± 0.3 mm × ±0.4 mm for 30 × 40 mm sensor size).

Under the assumption that point application load has no spread of subskin strain for thin pressure conductive rubber, the localization of the tactile sensor was assumed to be equal to the tactile element size. Sensitivity of both sensors is 100 gm/cm². However, with a better quality of pressure conductive rubber, it can be improved to 20 gm/cm².

Fig. 8. Schematic of gripper with tactile and centroid sensors.

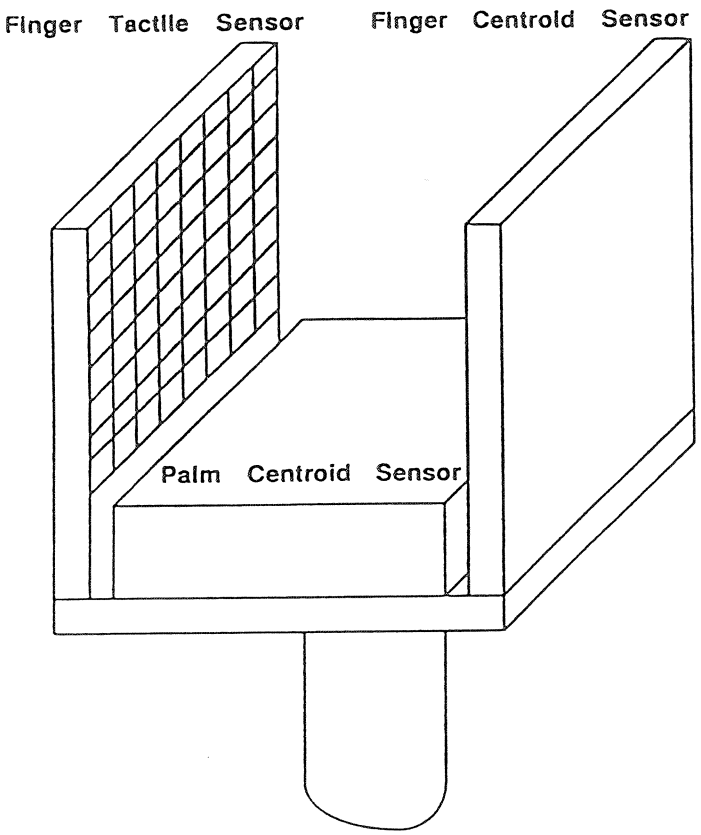

Fig. 9. Instrumented end-effector.

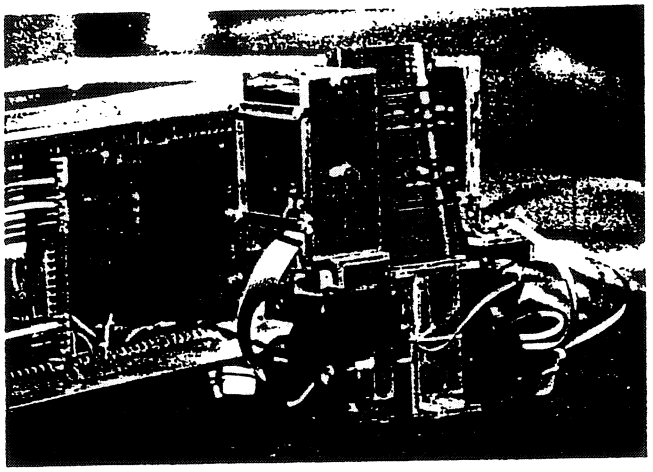

Fig. 9

Fig. 10. Sample matrix tactile sensor output.

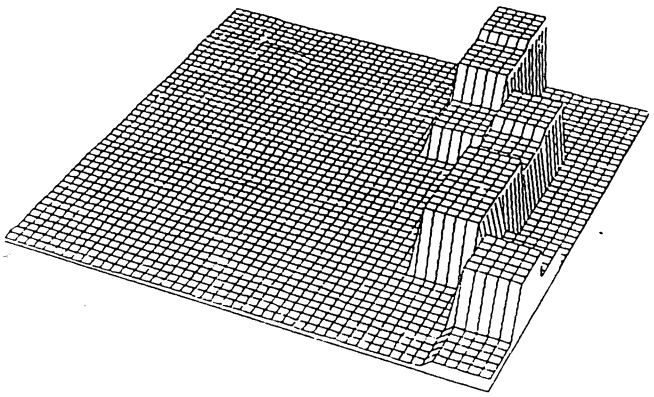

Fig. 10

5.2. Application

The placement error in the position and orientation of object, dimensional tolerance, and positioning error of the robot make the position of the object uncertain with respect to the gripper. Since such uncertainties cannot be determined ahead of time, a robust assembly program will use the sensory information in real time to update the position and orientation of the object.

We mounted on a two-degree-of-freedom parallel jaw gripper the tactile sensor on one finger, a centroid sensor on the other finger, and a centroid sensor on the palm (see Fig. 8). An example of a grasped object is shown in Fig. 9. The edge indentation on the 8×8 tactile sensor (see Fig. 10) gives a measurement of the object's edge. The two centroid sensors provide measurements of vertex contacts. For a grasped object of approximately 100 mm $\times$ 60 mm $\times$ 60 mm size, there are four measurements: two vertices from the two centroid sensors and two endpoints of a line from the tactile sensor. If all these four measurements are considered in pair, there are six features on the object that are matched. The orientation estimate obtained from matching all six measurements has a weighted maximum expected error of $\pm 7°$. By considering the three pairs corresponding to the set of *best features*, the weighted maximum expected error is reduced to $\pm 3°$. This algorithm runs in real time at 10 Hz under the NYMPH multiprocessor system (Chen et al. 1986).

6. Conclusion

In this paper, a framework for the integration of multiple sensors to determine the position and orientation of an object has been proposed. We have defined *best features* in the sense of determining best estimate of these parameters. The orientation parameters are nonlinear functions of device measurements. Since the error in the estimate of orientation parameters depends on the spatial distribution of the measurements and the device error, some combination of measurements have small expected error. The best estimate is obtained by solving the system of *best features* in a weighted least squares sense. The maximum expected error on the estimate has also been determined. The algorithm is computationally efficient for real-time application. The results have been substantiated using an end-effector instrumented with a matrix tactile sensor and two centroid sensors.

Acknowledgments

Support for this work has been provided by a grant from AFOSR under contract F49620-82-C-0092, the National Science Foundation under contract MEA80-19628, and by a grant from the System Development Foundation. The authors would like to thank Brian Armstrong, Ron Fearing, and Vishvjit Nalwa for their invaluable assistance.

Appendix: Quaternions

Let (u_0, u_1, u_2, u_3) be the components of the quaternion

$$\mathbf{q} = u_0 + \mathbf{i}u_1 + \mathbf{j}u_2 + \mathbf{k}u_3. \qquad (A.1)$$

A convenient representation of quaternions uses a scalar u_0 and a vector $\mathbf{u} = \mathbf{i}u_1 + \mathbf{j}u_2 + \mathbf{k}u_3$:

$$\mathbf{q} = (u_0, \mathbf{u}). \qquad (A.2)$$

The addition and product on quaternions are defined by

$$\begin{aligned} \mathbf{q} + \mathbf{q}' &= (u_0 + u_0') + \mathbf{i}(u_1 + u_1') \\ &\quad + \mathbf{j}(u_2 + u_2') + \mathbf{k}(u_3 + u_3'), \\ \mathbf{q}\mathbf{q}' &= (u_0u_0' - \mathbf{u}\cdot\mathbf{u}', \mathbf{u}\times\mathbf{u}' + u_0\mathbf{u}' + u_0'\mathbf{u}). \end{aligned} \qquad (A.3)$$

The conjugate or inverse of a quaternion is

$$\mathbf{q}^* = (u_0, -\mathbf{u}). \qquad (A.4)$$

Quaternions can be used to represent rigid body rotation. The components of quaternion $\mathbf{q}$ are the set of four Euler parameters. The set of Euler parameters for rotation about a vector $\mathbf{r}$ of an angle θ or about $-\mathbf{r}$ of an angle $-\theta$ are

$$u_0 = \cos(\theta/2), \qquad \mathbf{u} = \sin(\theta/2)\mathbf{r}, \qquad (A.5)$$

with

$$u_0^2 + u_1^2 + u_2^2 + u_3^2 = 1 \qquad (A.6)$$

The transformation of ${}^o\mathbf{v}$ to ${}^s\mathbf{v}$ as in Eq. (2) is effected in quaternion algebra by the operation

$${}^s\mathbf{v}_i = \mathbf{q}\,{}^o\mathbf{v}_i\,\mathbf{q}^*, \qquad (A.7)$$

where ${}^o\mathbf{v}_i$ and ${}^s\mathbf{v}_i$ are equivalent to the quaternions $(0, {}^o\mathbf{v}_i)$ and $(0, {}^s\mathbf{v}_i)$.

References

Bolle, R. M., and Cooper, D. B. 1986. On optimally combining pieces of information, with application to estimating 3-D complex-object position from range data. *IEEE Trans. on Pattern Analysis and Machine Intelligence* 8(5):619–638.

Brooks, R. A. 1982. Symbolic error analysis and robot planning. *Int. J. Robotics Res.* 1(4):29–68.

Chen, J. B. et al. 1986 (San Francisco). NYMPH: A multiprocessor for manipulation application. *Proc. IEEE Int. Conf. on Robotics and Automation*, pp. 1731–1736.

Faugeras, O. D., and Hebert, M. 1983 (Los Altos, Calif.). A 3-D recognition and positioning algorithm using geometri-

cal matching between primitive surfaces. *Proc. Eighth Int. Joint Conf. on Artificial Intelligence,* pp. 996–1002.

Grimson, W. E. L., and Lozano-Perez, T. 1984. Model based recognition and localization from sparse range or tactile data. *Int. J. Robotics Res.* 3(3):3–35.

Ishikawa, M., and Shimojo, M. 1982. A method for measuring the center position of a two dimensional distributed load using pressure conductive rubber. *Transaction SICE* 18(7):730–735.

Khatib, O. 1980. Commande dynamique dans l'espace opérationnel des robots manipulateurs en présence d'obstacles. Thése de Docteur-Ingénieur. École National Supérieure de l'Aéronautique et de l'Espace, Toulouse, France.

Popplestone, R. J., Ambler, A. P., and Bellow, I. 1980. An interpreter for a language for describing assemblies. *Artificial Intelligence* 14:79–107.

Shimojo, M., and Ishikawa, M. 1985a. A custom hybrid IC for sensory data transmission. *Proc. Twenty-fourth SICE,* pp. 137–138.

Shimojo, M., and Ishikawa, M. 1985b. A tactile sensor including proximity and thermo detector. *Proc. Twenty-eighth Joint Conf. on Automatic Control,* pp. 419–420.